

Output characteristics of weak-coupling fiber grating external cavity semiconductor laser

H. ZHOU¹, G. XIA^{1,2}, Y. FAN^{1,3}, T. DENG¹, and Z. WU^{*1,2}

¹School of Physics, Southwest Normal University, Chongqing 400715, China

²The Key Laboratory for Optoelectronic Technology & System, Ministry of Education, Chongqing University, Chongqing 400044, China

³School of Science, Southwest University of Science and Technology, Mianyang 621002, China

After taking into account the contribution of fiber grating to the phase condition, the mode distribution of fiber grating external cavity semiconductor laser (FGESL) has been determined, and the output characteristics of weak-coupling fiber grating external cavity semiconductor laser (WCFGESL) have been investigated theoretically through solving the multi-mode rate equations numerically. The results show that with increase in the injected current, the lasing wavelength of WCFGESL appears fluctuation, whose amplitude is influenced by the external cavity length to a certain degree, the side mode suppression ratio (SMSR) increases accompanied by an oscillation, and the P-I curve distorts slightly. All these theoretical estimations accord with the reported experimental observations.

Keywords: weak-coupling fiber grating external cavity semiconductor laser, lasing wavelength, side mode suppression ratio.

1. Introduction

Successful implementation of dense wavelength division multiplexed (DWDM) optical networks will depend deeply on the availability of low-cost, stable single-longitudinal mode and narrow line-width laser sources. In recent years, fiber grating external cavity semiconductor laser (FGESL) has received considerable attention as a promising source to satisfy these strict requirements [1–10]. A FGESL consists of a laser diode (LD) chip and a fiber grating (FG) external cavity, where the FG acts as the wavelength selective device. In order to improve the single-mode selectivity of the FGESL, it is customary to apply anti-reflection (AR) coating to the LD front facet (i.e., the facet facing to the FG external cavity). However, the AR coating approach makes the fabrication process complicated. Thus, the non-AR-coated FGESL, which is usually called as weak-coupling FGESL (WCFGESL), has attracted attention. Also the output characteristics of the WCFGESL have been preliminary studied experimentally and theoretically [1–4], and some experimental phenomena such as the fluctuation of the lasing wavelength and the side mode suppression ratio (SMSR) with the injected current, the distortion of the P-I curve, have been observed. However, the related theoretical description is inadequate and cannot explain these phenomena with satisfaction. We have noticed that the adopted theoretical models in these investigations neglected the

contribution of fiber grating to the phase condition, which obviously deviates from the physical facts. Based on above consideration, in this paper, the mode distribution of FGESL is determined after taking into account the contribution of the FG to the phase condition, and the output characteristics of WCFGESL have been investigated theoretically through solving the multi-mode rate equations numerically.

2. Theory

A FGESL is composed of a laser diode (LD) chip with the length L_d and a FG external cavity with the length L_f . The reflectivity of the front facet of the diode, the other facet of the diode, and the FG, is R_2 ($= r_2^2$, r_2 is the reflection coefficient), R_1 ($= r_1^2$, r_1 is the reflection coefficient), and $R_g(\lambda)$ ($= |r_g(\lambda)|^2$, $r_g(\lambda)$ is the reflection coefficient), respectively. Usually, an equivalent cavity model can be adopted to analyse the characteristics of the FGESL [9], where the front facet and the FG can be combined and represented with an equivalent reflectivity $R_e(\lambda)$ ($= |r_e(\lambda)|^2$, $r_e(\lambda)$ is equivalent reflection coefficient).

Taking the multi-reflected effect of light inside the external cavity into account, the equivalent reflection $r_e(\lambda)$ of the FG external cavity can be expressed as

$$r_e(\lambda) = \frac{r_2 + \eta r_g(\lambda) \exp(-ip)}{1 + \eta r_2 r_g(\lambda) \exp(-ip)}, \quad (1)$$

* e-mail: zmwu@swnu.edu.cn

where λ is the wavelength, η is the coupling efficiency between the LD and the fiber, ρ is the round trip phase delay of the external cavity. If a uniform FG has been used, $r_g(\lambda)$ can be decided by [11]

$$r_g(\lambda) = \frac{i\kappa \sin(qL_g)}{q \cos(qL_g) - i\delta\beta \sin(qL_g)}, \quad (2)$$

where L_g is the FG length, κ is the coupling coefficient, $q = [(\delta\beta)^2 - \kappa^2]^{1/2}$ and $\delta\beta = \beta(\lambda) - \beta_g$ is the detuning of light from exact Bragg resonance. In order to simplify the expression, $r_g(\lambda)$ can be divided into the following phase and amplitude formulation, i.e.,

$$r_g(\lambda) = |r_g(\lambda)| \exp(i\theta) = r(\lambda) \exp(i\theta). \quad (3)$$

Then, combining Eqs. (1)–(3), the FG external cavity equivalent reflectivity $R_e(\lambda)$ can be obtained.

For a steady-state FGESL, within the frame of the mean field approximation, the multi-mode rate equations can be written as

$$0 = \frac{dN}{dt} = \frac{I}{eV} - \frac{c}{n_d(I)} \sum_m g_m S_m - \frac{N}{\tau_s}, \quad (4a)$$

$$0 = \frac{dS_m}{dt} = \frac{c}{n_d(I)} \left(\Gamma g_m - \left[\alpha + \frac{1}{2L_d} \ln\left(\frac{1}{R_1 R_e}\right) \right] \right) S_m + \frac{\Gamma \gamma N}{\tau_s}, \quad (4b)$$

where I is the injected current, e is the electron charge, V is the volume of an active layer, c is the light velocity in the vacuum, τ_s is the spontaneous emission lifetime, N is the carrier density, Γ is the optical confinement factor, α is the loss coefficient, S_m is the photon density of the m^{th} mode, γ is the spontaneous emission factor, and g_m is the gain of the m^{th} mode, which can be expressed as

$$g_m = a \left[\frac{N}{1 + (\lambda_p - \lambda_m)^2 / Q_g^2} - N_0 \right], \quad (5)$$

where a is the differential gain coefficient, N_0 is the transparency carrier density, λ_p is the peak wavelength of the gain, Q_g characterizes the width of gain, and λ_m is the resonant wavelength of the m^{th} mode, which should satisfy the phase condition

$$r_2 r_1 G \sin \phi + \eta r_2 r(\lambda) \sin(\rho - \theta) - \eta r_1 r(\lambda) \times G \sin(\phi + \rho - \theta) = 0 \quad (6)$$

where ϕ is the round trip phase delay of the LD, G is the net gain factor which can be expressed as

$$G = \exp[(\Gamma g_m - \alpha)L_d], \quad (7)$$

The $n_d(I)$ in Eq. (4) is the refractive index of the gain medium under the injected current I , whose variation with I can be described as [2]

$$n_d(I) = n_{d0} + k(I - I_0), \quad (8)$$

where I_0 is the reference current, n_{d0} is the refractive index of the gain medium under I_0 , and k is the varying slope efficiency of the refractive index of gain medium with I .

Based on the above analysis, for a FGESL of given parameters, the S_m can be specified and the output power of the m^{th} mode can be calculated by

$$P_m = \frac{(1 - R_e) \sqrt{R_1}}{(1 - R_e) \sqrt{R_1} + (1 - R_1) \sqrt{R_e}} \frac{hc}{\lambda_m} \frac{c}{n_d} \times \left(\frac{1}{2L_d} \ln \frac{1}{R_1 R_e} \right) V S_m, \quad (9)$$

where h is the Planck's constant.

The side mode suppression ratio (SMSR), which is an important parameter measuring the spectral purity of a laser, can be defined as

$$\text{SMSR} \equiv 10 \lg \left(\frac{P_0}{P_1} \right), \quad (10)$$

where P_0 is the peak mode power and P_1 is the power with the most intense side mode.

Based on above expressions, the output characteristics of a FGESL can be investigated numerically.

3. Results and discussions

The calculated output characteristics of WCFGESL as a function of injected current have been given in Fig. 1, where Figs. 1(a)–1(c) are for lasing wavelength, SMSR and output power, respectively. The used fiber grating in calculations, whose length L_g is about 6 mm, has a maximum reflectivity 80% at the centre wavelength of 1552 nm with a 3-dB bandwidth of 0.2 nm. The other data used in calculations are: $n_f = 1.44$, $L_f = 8$ mm, $L_d = 380$ μm , $n_{d0} = 3.4$, $I_0 = 20$ mA, $k = 0.58$ A^{-1} , $R_1 = 0.92$, $R_2 = 0.3$, $\Gamma = 0.3$, $N_0 = 1.0 \times 10^{18}$ cm^{-3} , $\alpha = 40$ cm^{-1} , $Q_g = 20$ nm, $a = 2.5 \times 10^{-16}$ cm^2 , $c = 3.0 \times 10^8$ m/s, $\tau_s = 3.0$ ns, $\gamma = 5 \times 10^{-5}$, $e = 1.6 \times 10^{-19}$ C, $V = 1.2 \times 10^{-10}$ cm^3 , $\lambda_p = 1552$ nm, $\eta = 0.5$, $\kappa = 242.2$ m^{-1} , and $h = 6.63 \times 10^{-34}$ Js.

In Fig. 1(a), with the increase in the injected current, the lasing wavelength appears fluctuation around the FG Bragg reflection wavelength. Based on above theory, it can be discovered that after taking into account the contribution of the FG to the phase condition, the resonant mode distribution of WCFGESL is very complex and the mode spacing between a mode and the adjacent mode is no longer equal. The change of the injected current will result in vari-

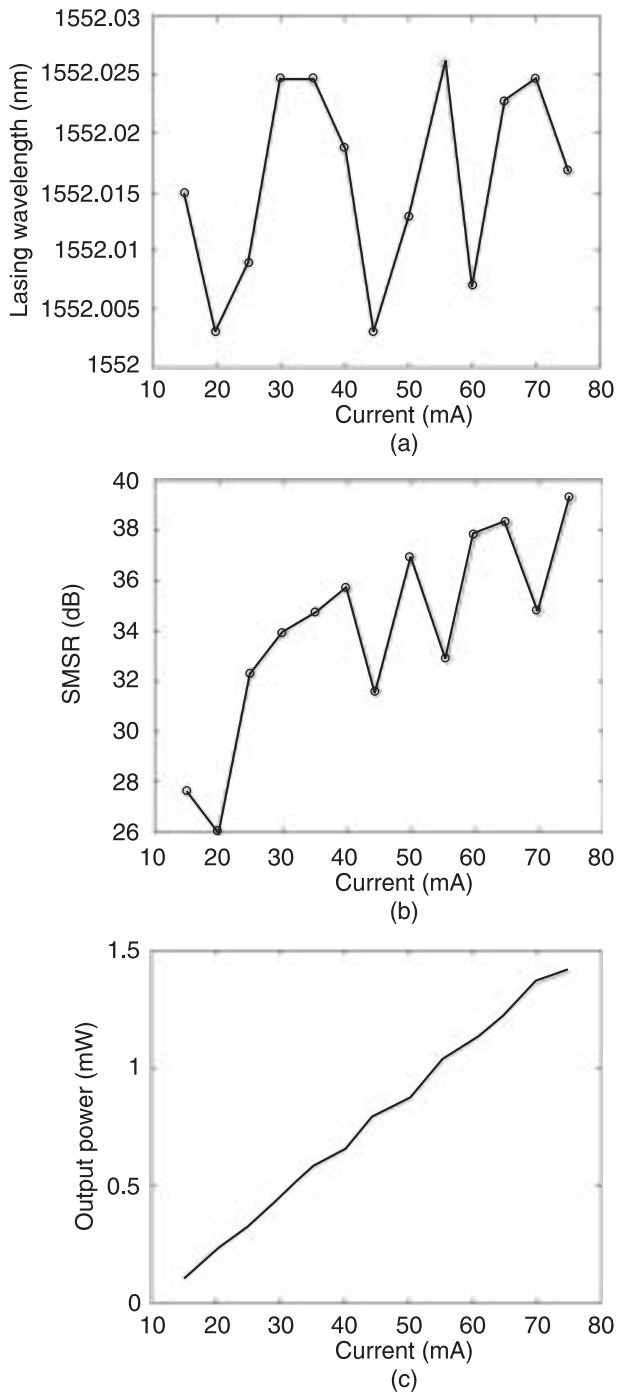


Fig. 1. The calculated output characteristics of WCFGESL as a function of injected current, where Figs. (a), (b), and (c) are for lasing wavelength, SMSR and output power, respectively.

ation of the refractive index of the LD medium and furthermore the resonant mode wavelength, which results in the fluctuation of the lasing wavelength of the WCFGESL.

It can be seen from Fig. 1(b) that with the increase in the injected current, the SMSR of the WCFGESL increases accompanied by an oscillation. On one hand, as the injected current increases, the carrier density will increase and the mode competition will induce the more violent suppression of the main mode to the side mode, which makes

the SMSR behave an increasing tendency. On the other hand, as mentioned above, along with the injected current increasing, the mode distribution will vary. Owing to the contribution of the FG, the most intense side mode may no longer be the mode nearest to the peak mode, and the wavelength interval between the peak mode and the most intense side mode maybe change (increase or decrease) with the change of the injected current. After taking into account the wavelength dependence of the gain profile of the LD medium, an oscillation of the SMSR with the injected current can be comprehended. The joint action of above two factors make the SMSR behave as Fig. 1(b) with the injected current increasing. For example, when the injected current increases from 40 mA to 45 mA, the SMSR should increase if only the mode suppression effect is considered. However, the mode distribution changes at the same time, and the calculated results show that the wavelength interval between the peak mode and the most intense side mode under 45 mA is about 0.04 nm, which is smaller than that under 40 mA (about 0.37 nm). Under this circumstance, the SMSR will decrease. The joint contribution of the two factors makes the SMSR under 45 mA be smaller than that under 40 mA.

Figure 1(c) shows the P-I curve of the WCFGESL. The P-I curve of a semiconductor laser is usually approximately linear. However, this linearity may be lost in the WCFGESL, and the variation of the mode distribution with the injected current is responsible for the distortion of the P-I curves.

All above numerical simulations are to a certain degree in agreement with the experimental observation by other researchers, which show the rationality of the model adopted in this paper.

In practical applications, different fiber external cavity length L_f is adopted in the FGESL. In Fig. 2, the variation of lasing wavelength of the WCFGESL with injected current for $L_f = 1$ mm and $L_f = 10$ mm has been plotted. It can be seen from this diagram that the external cavity length has an obvious influence on the fluctuation amplitude of the lasing wavelength. With the increase in the external cavity length, the current-dependent lasing wavelength fluctuation amplitude becomes small. This can be explained as that, though the mode spacing is unequal in WCFGESL, a short external cavity has a relatively narrow mode spacing than a long external cavity, which will inevitably result in a larger oscillation of the lasing wavelength for a short external cavity than that for a long external cavity after considering the longitudinal mode distribution change and the gain profile of the LD medium. When the external cavity become even longer, the mode spacing is so small that the variation of the lasing wavelength cannot be clearly distinguished in a figure, so we have not given the case for $L_f > 10$ mm. Meanwhile, it can be seen in this diagram that the lasing wavelength of short external cavity WCFGESL may escape from the fiber grating 3 dB reflection window under several injected currents which has been observed in experiments [1,2]. The reason is that the

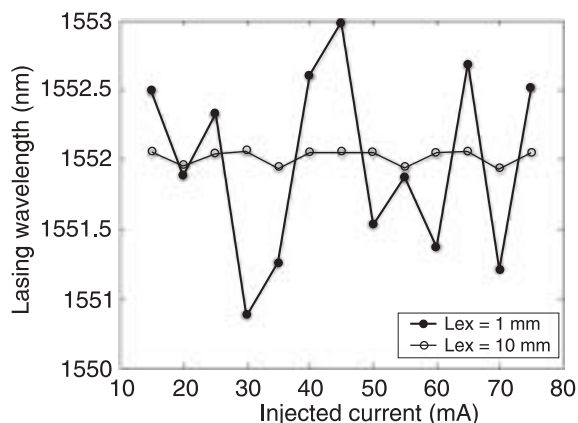


Fig. 2. Variation of the lasing wavelength with injected current for two external cavity lengths.

joint contribution of LD, external cavity and FG to the phase condition, may cause no one resonant wavelength within the fiber grating 3-dB reflection window under those injected currents, or though there exist several resonant modes within the fiber grating 3-dB reflection window, the obtained gains of these mode may be smaller than that of some mode outside the fiber grating 3 dB reflection window.

Acknowledgements

This work received the support from the Key Project of Chinese Ministry of Education (No. 03140) and the Commission of Science and Technology of Chongqing City of China.

References

1. T.S. Lay, M.H. Chen, H.M. Yang, and W.H. Cheng, "1.55- μ m fiber grating laser utilizing an uncoated tapered

- hemispherical-end fiber microlens", *Jpn. J. Appl. Phys.* **42**, 453–455 (2003).
2. T.S. Lay, M.H. Chen, H.M. Yang, S.H. Wu, and W.H. Cheng, "1.55- μ m non-anti-reflection-coated fiber grating laser for single-longitudinal mode operation", *Opt. & Quantum Electron.* **34**, 687–696 (2002).
3. J. Geng, G. Cao, Y. Luo, R. Qu, G. Chen, Z. Fang, and X. Wang, "Experimental study of a fiber grating external-cavity semiconductor laser", *Chinese J. Lasers* **A27**, 488–492 (2000). (in Chinese).
4. L. Xue, H. Zhao, X. Li, and Y. Ye, "Characteristics of the FBG external cavity semiconductor laser with weak feedback", *Chinese J. Lasers* **A28**, 877–880 (2001). (in Chinese).
5. W.H. Cheng, S.F. Chiu, C.Y. Hong, and H.W. Chang, "Spectral characteristics for a fiber grating external cavity laser", *Opt. & Quantum Electron.* **32**, 339–348 (2000).
6. K. Zhou, X. Hu, H. Liu, H. Ge, and G. An, "Fiber grating external cavity semiconductor laser with narrow linewidth high MSR". *Acta Photonica Sinica* **30**, 478–482 (2001). (in Chinese).
7. F.N. Timofeev, G.S. Simin, M. S. Shatalov, S. A. Gurevich, P. Bayvel, R. Wyatt, I. Lealman, and R. Kashyap, "Experimental and theoretical study of high temperature-stability and low-chirp 1.55- μ m semiconductor laser with an external fiber grating", *Fiber & Integrated Optics* **19**, 327–353 (2000).
8. T. Kato, T. Takagi, A. Hamakawa, K. Iwai, and G. Sasaki, "Fiber-grating semiconductor laser modules for dense-WDM systems", *IEICE Trans. Electron.* **E82-C**, 357–359 (1999).
9. Z. Wu and G. Xia, "Oscillation wavelength of fiber Bragg grating semiconductor lasers", *Optik* **113**, 348–350 (2002).
10. R.J. Campbell, J.R. Armitage, G. Sherlock, O.L. Williams, R. Payne, M. Robertson, and R. Wyatt, "Wavelength stable uncooled fiber grating semiconductor laser for use in an all optical WDM access network", *Electron. Lett.* **32**, 119–120 (1996).
11. G.P. Agrawal, *Nonlinear Fiber Optics*, Academic, New York, 1995.